Spectrochimica Acta Part A: Molecular and Biomolecular Spectroscopy 140 (2015) 74–84

Contents lists available at ScienceDirect

Spectrochimica Acta Part A: Molecular and Biomolecular Spectroscopy

journal homepage: www.elsevier.com/locate/saa

Reactivity and molecular modeling of new solvatochromic mixed-ligand copper(II) chelates of 2-acetylbutyrolactone and dinitrogen bases

A. Taha, Omima M.I. Adly *, Magdy Shebl

Department of Chemistry, Faculty of Education, Ain Shams University, Roxy, Cairo 11711, Egypt

HIGHLIGHTS

- Solvatochromic Cu(II)-chelates.
- Mononuclear mixed ligand chelates.
- Specific and non-specific solvent interactions with metal chelates.
- Molecular modeling of free ligands and their chelates has been calculated.

GRAPHICAL ABSTRACT

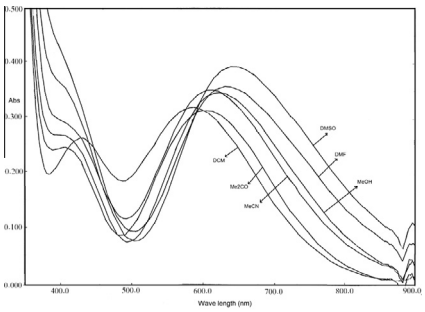

ARTICLE INFO

Article history:
Received 26 August 2014
Received in revised form 1 November 2014
Accepted 20 November 2014
Available online 13 December 2014

Keywords:
Mixed ligand
Lewis acid–base
Solvatochromic
Specific and non-specific interactions
Molecular modeling

ABSTRACT

A new series of solvatochromic mononuclear mixed ligand chelates with the general formula: Cu(AcBL)(L)X; where AcBL = 2-acetylbutyrolactonate, L = N,N,N′,N′-tetramethylethylenediamine (Me_4en), N,N,N′,N′-tetramethylpropylene diamine (Me_4pn), 1,10-phenanthroline (Phen) or 2,2′-bipyridyl (Bipy) and X = ClO_4^-, NO_3^- or Br^- have been synthesized and characterized by the analytical and spectral methods, as well as magnetic and molar conductance measurements. The d–d absorption bands of Me_4en-chelates as Nujol mulls or weak donor solvents solutions revealed square-planar, distorted octahedral and/or distorted trigonal bipyramid geometries for the perchlorate, nitrate and bromide chelates, respectively. However, an octahedral structure is identified for chelates in strong donor solvents. Perchlorate chelates show a remarkable color change from violet to green as the Lewis basicity of the donor solvent increases, whereas bromide chelates are mainly affected by the Lewis acidity of solvent. Specific and non-specific interactions of solvent molecules with the chelates were investigated on the basis of unified solvation model. Structural parameters of the free ligands and their Cu(II)-chelates have been calculated on the basis of semiempirical *PM3* level and correlated with the experimental data.

1. Introduction

Solvatochromism is commonly used in many fields of chemical and biological research to study bulk and local polarity in macrosystems (membranes, etc.), notwithstanding its wide use, and still remains a largely unknown phenomenon due to the enormously complex coupling of many different interactions and dynamical processes which characterize it. Metal–chelates with O_2N_2 mixed ligands have been studied as Lewis acid-base indicators [1–5]. Since 2-acetylbutyrolactone (HAcBL) is used as an intermediate for the synthesis of various organic chemicals especially that most widely used as therapeutic agents. They are useful in treatment of rheumatoid arthritis and some inflammatory diseases [6,7]. In addition, some furanone derivatives displayed a good anti-neoplastic activity and high selectivity against some cell lines from

* Corresponding author. Tel.: +20 1008693220.
E-mail address: omima_adly@yahoo.com (O.M.I. Adly).

http://dx.doi.org/10.1016/j.saa.2014.11.056
1386-1425/

leukemia, lung cancer, colon and melanoma panels that might enhanced after chelation with metal ions [8]. In view of the limited information available regarding the spectroscopic properties of mixed ligand metal chelates containing HAcBL, the present study is a continuation of our studies on the chromotropic of mixed metal chelates of ligands containing O–O and N–N in various solvents [9–13]. This study was undertaken to analyze the influence of different solvents on the UV/Vis spectra of chelates to achieve a microscopic understanding of the intermolecular effects. Hence, the main goal of this study is to examine the reactivity and applicability of the current complexes as a Lewis acid-base color indicator. For this purpose a new series of copper(II) chelates abbreviated as Cu(AcBL)(L)X; where: AcBL = 2-acetylbutyrolactonate, L = diamine: Me_4en, Me_4pn or diimine: Phen or Bipy; and X = ClO_4^-, NO_3^- or Br^- were prepared and characterized on the basis of Micro-analytical, spectral, magnetic and molar conductance measurements. Furthermore, the molecular orbital modeling has been performed based for the proposed structures on semiempirical *PM3* level to recognize the structural parameters of the current compounds in molecular terms and correlate with their experimental results.

2. Experimental

2.1. Materials

All chemicals are of the analytical reagent grade, obtained from either Merck or Aldrich and used without further purification. The solvents, dichloromethane (CH_2Cl_2), nitromethane ($MeNO_2$), acetonitrile (MeCN), acetone (Me_2CO), methanol (MeOH), ethanol (EtOH), N,N-dimethylformamide (DMF), dimethylsulfoxide (DMSO) and pyridine (py) were further purified as described elsewhere [13].

2.2. Physical measurements

Infrared spectra were recorded in the region (4000–400 cm^{-1}) on a Shimadzu FTIR 8101 spectrophotometer as KBr pellets. Electronic spectra of the chelates in solution or as Nujol mulls were recorded at room temperature using UV-2101 pc w/full spectrophotometer. The molar conductance at 25 °C was measured for chelates solutions in DMF with Metrohm 660 conductivity bridge. Magnetic moments of chelates were obtained using a MSB-AUTO magnetic susceptibility balance by the Gouy method and effective magnetic moments were calculated [14].

2.3. Molecular modeling

An attempt to gain a better insight on the molecular structure of ligands and their chelates, geometric optimization and conformation analysis has been performed on the basis of semiempirical *PM3* force field as implemented in *hyperchem 7.52* software [15].

2.4. Syntheses of Cu(AcBL)(L)X chelates

To an ethanolic solution of 5 mmol of an appropriate $CuX_2{\cdot}nH_2O$ (X = ClO_4^- or NO_3^-), a solution of HAcBL ligand in 20 mL ethanol was added dropwise with a continuous stirring, meanwhile 10 mmol of anhydrous Na_2CO_3 was added in small portions. The mixture was continuously stirred for about 30 min. until a greenish solution was obtained and then filtered. A solution of 5 mmol of the secondary diamine or diimine ligand (L) in 10 mL EtOH was added dropwise to the filtrate with continues stirring for an additional half an hour. Either, a solution or a precipitate that filtered off and left to stand overnight. The chelates obtained were re-crystallized from CH_2Cl_2 solvent and stored in a desiccator over $CaCl_2$.

Table 1
Colors, analytical data, d–d absorption frequencies in Nujol mulls, molar conductance, and magnetic moments of Cu(II) complexes.

	Ligand/complex	Molecular formula	M.P °C	M. Wt. Yield (%)	Color	Elemental analyses found (calcd.)%			λ_{max}/nm[a]	Λ/S.cm^2 Mol^{-1} (DMF)	$\mu_{eff.}$ (B.M)
						C	H	N			
(**1**)	[Cu(AcBL)(Me$_4$en)]ClO$_4$	($C_{12}H_{23}N_2O_7Cl$)Cu	>300	406 (70.3)	Bluish violet	34.72 (35.47)	5.32 (5.71)	6.72 (6.90)	585	75.2	1.66
(**2**)	[Cu(AcBL)(Me$_4$en)NO$_3$]	($C_{12}H_{23}N_3O_6$)Cu	>300	368.5 (58.5)	Blue	37.87 (39.06)	6.16 (6.29)	11.44 (11.39)	629	77.8	1.72
(**3**)	[Cu(AcBL)(Bipy)]ClO$_4$	($C_{16}H_{23}N_2O_7Cl$)Cu	>300	454.18 (61.7)	Olive green	43.07 (42.27)	4.87 (5.11)	6.35 (6.17)	621	56.5	1.63
(**4**)	[Cu(AcBL)(Phen)]ClO$_4$	($C_{18}H_{15}N_2O_7Cl$)Cu	>300	470.2 (77.5)	Green	45.82 (45.96)	3.08 (3.22)	6.21 (6.36)	622	79.6	1.69
(**5**)	[Cu(AcBL)(Me$_4$Pn)]ClO$_4$	($C_{13}H_{25}N_2O_7Cl$)Cu	>300	420 (62.7)	Green	38.06 (37.13)	5.85 (6.00)	6.23 (6.67)	674	insol	1.82

[a] The d–d absorption frequencies are measured in Nujol mulls.

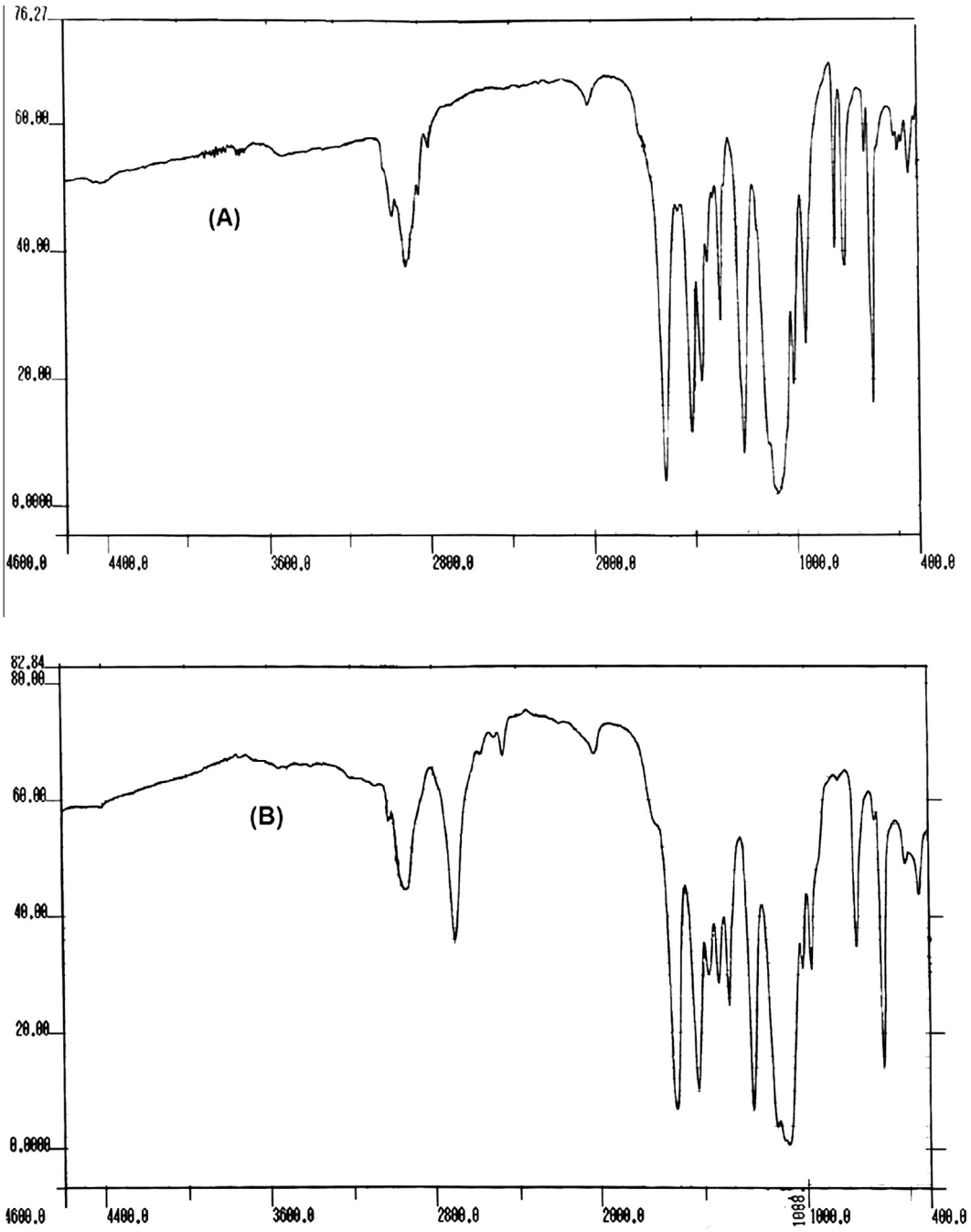

Fig. 1. Infrared spectra of Cu(AcBL)(Me_4en)]ClO_4 **1** (A) and [Cu(AcBL)(Me_4Pn)]ClO_4 **5** (B).

Table 2
Wavenumbers/cm^{-1} of the main absorption bands of the infrared spectra of Cu(AcBL)(NN)X complexes.

	Ligand/ complex	ν(C=O) lactone	ν(C=C)	$\nu(ClO_4)$		ν(M–N)	ν(M–O)	Other band
	HAcBL	1771 s	–	–	–	–	–	–
(**1**)	[Cu(AcBL)(Me_4en)]ClO_4	1644 s	1514 s	1102, 1017	623	515 w	442 w	–
(**2**)	[Cu(AcBL)(Me_4en) NO_3]	1644 s	1505 s	–	–	498 w	428 w	1385, 1262, 806 unidentate $\nu(NO_3)$
(**3**)	[Cu(AcBL)(Bipy)]ClO_4	1601 s	1580 s	1160, 1088	627	490 w	450 w	
(**4**)	[Cu(AcBL)(Phen)]ClO_4	1636 s	1586 s	1113, 1069	623	504 w	453 w	–
(**5**)	[Cu(AcBL)(Me_4Pn)]ClO_4	1636 s	1532 s	1146, 1019	629	513 w	448 w	–

s = strong, w = weak, br = broad.

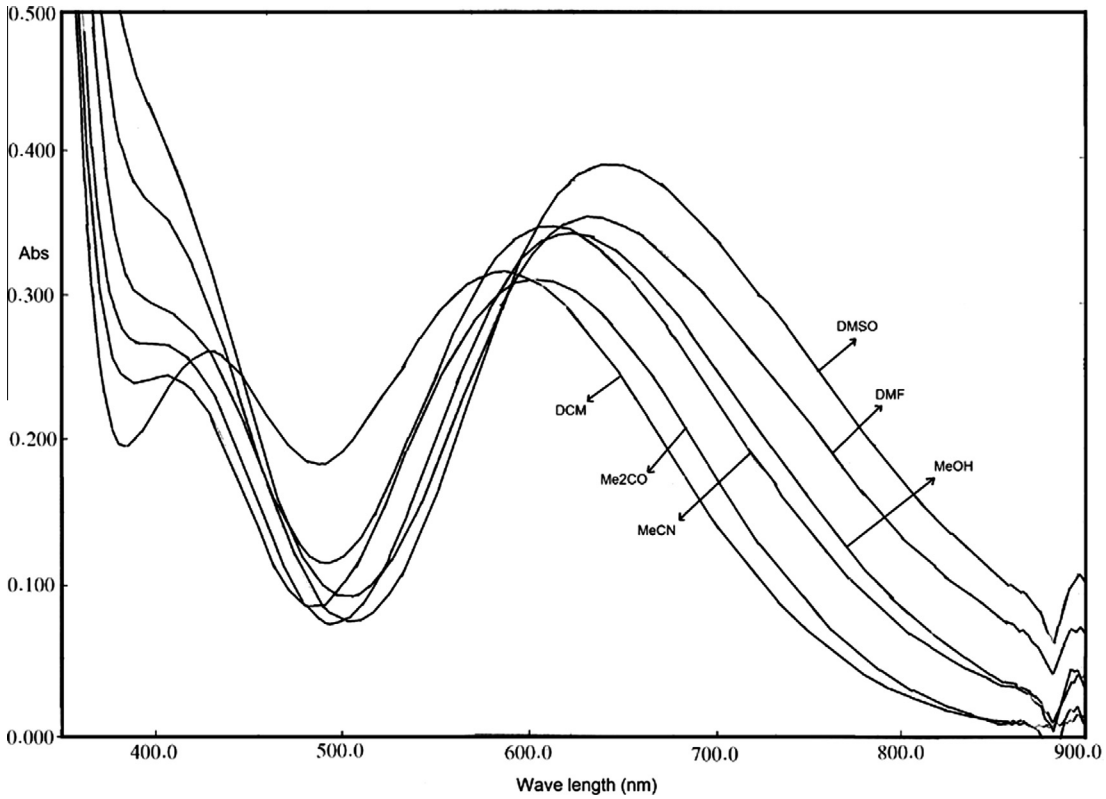

Fig. 2. Electronic absorption spectra of 4.0×10^{-3} mol L^{-1} of $[Cu(AcBL)(Me_4en)]ClO_4$ complex in different solvents; CH_2Cl_2, Me_2CO, MeCN, MeOH, DMF and DMSO, respectively, at 25 °C.

Table 3
Absorption maxima bands, λ_{max}/nm for the Cu(AcBL)(Me4en)X complexes solutions in various organic solvents at 25 °C.

	Complex	Py	DMSO	DMF	MeOH	Me_2CO	MeCN	$MeNO_2$
(**1**)	$[Cu(AcBL)(Me_4en)]ClO_4$	667	645	634	619	604	612	567
(**2**)	$[Cu(AcBL)(Me_4en)NO_3]$	681	652	640	620	626	622	618
(**6**)	$[Cu(AcBL)(Me_4en)$ Br]	–	674	708	632	730	708	714

[(6)]Br complex is formed in $MeNO_2$ solution by mixing Bu_4NBr with the perchlorate complex, **1** in a ratio (5:1).

The bromide chelate was prepared *in situ* by stirring a mixture of perchlorate chelate **1** with Bu_4NBr nitromethane solutions in a ratio 1:3 for 15 min. such as described earlier [9].

3. Results and discussion

The analytical and physicochemical data of the prepared chelates are given in Table 1. The obtained chelates are bluish-violet and greenish crystals for Me_4en- and Me_4pn or diimine-Cu(II) mixed ligand chelates, **1**–**2** and **3**–**5**, respectively. The elemental analyses of the metal chelates agreed quite well with the speculated formulae.

3.1. Infra-red spectra

Fig. 1 shows a representative example of IR spectra of $[Cu(AcBL)(Me_4en)]ClO_4$ complex **1** and $[Cu(AcBL)(Me_4Pn)]ClO_4$ complex **5**. The significant IR spectral data of free ligand (HAcBL) and its copper(II) chelates with their tentative assignments are summarized in Table 2. The stretching frequencies bands of the free ligand (HAcBL) appeared at 1771 and 1719 cm^{-1} those assigned to $\nu(C{=}O_{\alpha\text{-pyrone}})$ and $\nu(C{=}O_{\text{acetyl group}})$.

The $\nu(C{=}O_{\alpha\text{-pyrone}})$ shifted to lower frequencies in the range 1644–1601 cm^{-1} due to the chelation while the $C{=}O_{\text{acetyl group}}$ was disappeared in the IR spectra of metal complexes due to tautomerization and deprotonation of OH proton indicate participation of OH group in chelation, in addition the olefinc C=C in the metal complexes were observed in the range 1586–1505 cm^{-1} [8–12,16].

The coordination modes of anions have been inferred from the IR data in Table 2. Two intense vibrational bands appeared in the ranges of (1176–1102) and (623–629) cm^{-1}, which may be ascribed to the anti-symmetric stretching and anti-symmetric bending vibration modes, respectively [12,17,18]. The partial splitting observed for the broad band at 1100 cm^{-1} indicates mixture modes for perchlorate anion. Suggesting, weakly or non-coordinated perchlorate anion to the central copper(II) ion, depending on the coordination ability of the secondary ligand (L) toward Cu(II). i.e., the degree of splitting of this band serves as a measure of the degree and mode of the coordination of perchlorate anion to the copper ion [16]. This interpretation further emphasized by the linearity of this degree of splitting ($\Delta\nu$) *versus* E_{LUMO} and E_{gap} of the secondary ligands yielding: E_{gap}/eV = 6.21 + 0.04 $\Delta\nu$ ClO_4, r = 0.97 (3 points except Me_4en) and E_{LUMO}/eV = −3.11 + 0.042 $\Delta\nu$ ClO_4, r = 0.95 (3 points, except Me_4en).

Table 4
Solvatochromic parameters of the Cu(II) complexes, using K-T, Gutmann's and Drag's models Eqs. (1)–(3).

	Chelate	K-T					MLRA Using Gutmann parameter, Eq. (2)				MLRA Using Drago parameter, Eq. (3)					Relative contrib. %	
		C_o	α	β	π	r	$\nu_s^0/10^3$	a	b	r	W	P	E	C	r	non-specific	Specific
(**1**)	[Cu(AcBL)(Me$_4$en)]ClO$_4$	17.52	0.45 (12.5)*	−2.92 (81.1)	0.23 (6.93)	0.99	17.79	−0.79 (97.53)	−0.02 (2.47)	0.97	18.01	−0.29	−0.43	−0.43	0.98	30.26	34.21	35.53
(**2**)	[Cu(AcBL)(Me$_4$en)NO$_3$]	16.60	0.42 (20.1)	−1.61 (77.03)	0.06 (2.87)	0.93	16.62	−0.42 (89.36)	−0.05 (10.64)	0.95	12.14	0.66	0.30	1.92	0.99	25.22	37.39	37.39
(**6**)	[Cu(AcBL)(Me$_4$en)Br]	11.26	2.57 (42.98)	0.52 (8.70)	2.89 (48.33)	1.00	12.78	0.05 (6.49)	0.72 (93.51)	0.99	17.48	−0.23	−0.26	−0.27	0.96	22.92	10.42	66.67

* Values in the parenthesis is represented the contribution percentage.

Complex **2**, showed two absorption bands at 1385 and 1262 cm^{-1}, indicating that the nitrate anion behaves as unidentate nature [16]. The new bands observed in the ranges (515–504 cm^{-1}) and (428–451 cm^{-1}) could be assigned to the ν(M–N) and ν(M–O), respectively [8,19].

3.2. Conductivity and magnetic moment measurements

The molar conductance data observed for solutions of the soluble chelates **1**–**4** at room temperature in DMF solutions (10^{-3} M), listed in Table 1, and are in the range expected for 1:1 electrolytes [20]. This finding seems to be contradicting with the IR data, that showed coordinated nitrate anion, this contradiction could be understood *via* the driven out of the nitrate anion by DMF solvent molecules; as a result of the higher basicity of DMF (DN = 26.6) compared to donor number of nitrate anions (DN_X = 19.0) [21].

The molar magnetic moments data of the investigated Cu(II) chelates are found in the range 1.63–1.82 B.M., which is consistent with one unpaired electron (d^9) [9].

3.3. Electronic spectra

Fig. 2 shows representative visible absorption spectra of the [Cu(AcBL)(Me$_4$en)]ClO$_4$ complex, **1** in different organic solvents. The electronic spectrum shows only one broad band in the visible region, corresponding to the transfer of an electron to the hole in $d_{x^2-y^2}$ orbital of the Cu(II) ion (d^9) [11]. Table 3 collects the d–d visible absorption spectral data in various solvents for the complexes **1**, **2** and bromide complex (**6**) which prepared *in situ*. However, the rest complexes are sparingly soluble in most organic solvents, thus the d–d bands of all chelates are recorded as Nujol mulls (Table 1).

The positions of the d–d absorption band of the Cu(AcBL)(Me$_4$-en)X, where X = perchlorate, nitrate and bromide anions in weak donor solvent (such as $MeNO_2$) are observed in the range 17,637, 16,181 and 14,000 cm^{-1}. These values could be assigned to the following d–d transitions: $d_{xy} \rightarrow d_{x^2-y^2}$ ($^2B_{1g} \rightarrow {}^2B_{2g}$), $d_{x^2-y2} \rightarrow d_{z^2}$ ($^2E_g \rightarrow {}^2T_{2g}$), and/or $d_{z^2} \rightarrow d_{x^2-y^2}$ [22]. These transitions suggest a square planar, distorted octahedral and/or square based pyramidal distorted trigonal bipyramide (SBPDTBP) geometries for perchlorate, nitrate and bromide chelates, respectively [23]. This could be attributed to the coordination abilities of these anions toward Cu(II). This interpretation is further confirmed by the linearity of the ν_{max}/cm^{-1} values in $MeNO_2$ solvent *versus* the donor strength of these anions ($DN_{X,MeNO2}$) [21], ν_{max}/cm^{-1} = 18,670–143.55 $DN_{X,MeNO2}$, r = 0.99. The −ve slope indicates blue shift analogous to the increase of anion's Lewis basicity (anionochromic), alike to that found for similar Cu(II)-chelates [9,23].

Chelates **1**–**2**, display solvatocromic "gradual color change from violet to green (red shift) as the donor strength of solvent increases", indicating donor–acceptor interactions. Multiple Linear Regression Analysis (MLRA) provides independent for this color changes. In this method, a dependent variables Y is described in terms of a series of explanatory variables X. In this respect, the well known Kamlet and Taft [24], donor–acceptor numbers (DN and AN) [25] and the unified solvation model of Drago [26–28] were used, according to Eqs. (1)–(3), respectively.

$$\nu_{max}/10^3\text{cm}^{-1} = \nu^{\circ} + c_1\alpha + c_2\beta + c_3\pi^* \quad (1)$$

$$\nu_{max}/10^3\text{cm}^{-1} = \nu^{\circ} + a(DN) + b(AN) \quad (2)$$

$$\nu_{max}/10^3\text{cm}^{-1} = W + P(S) + E_BE_A + C_BC_A \quad (3)$$

It is assumed that all the explanatory variables are independent of each other and truly additive as well as relevant to the problem

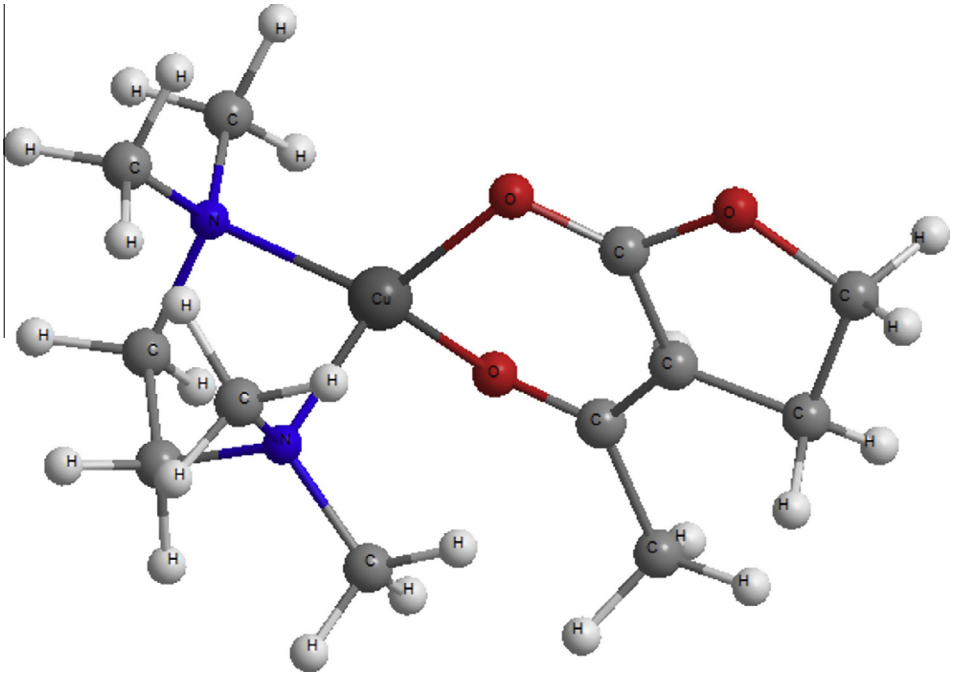

Fig. 3. Molecular modeling of $[Cu(AcBL)(Me_4en)]^+$ (**1**).

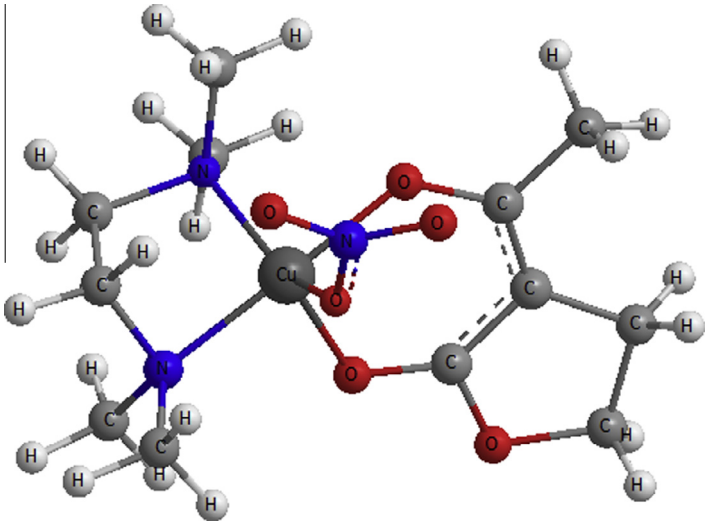

Fig. 4. Molecular modeling of $[Cu(AcBL)(Me_4en)NO_3]$ (**2**).

under study [28], where α reflects solvent H-bond donor (HBD), β reflects solvent H-bond acceptor (HBA) and π^* is the dipolarity-polarizability [25]. The corresponding *DN* and *AN* refer to the solvent Lewis basicity and acidity, respectively [22]. *S* is the solvent dipolarity term, *P* is a measure of the susceptibility of the complex to solvation. E_B, C_B and E_A, C_A quantify the electrostatic and covalent contributions to the Lewis basicity and acidity, respectively [26–28]. For acceptor probes, (chelates **1** and **2**), E_B and C_B solvent parameters are used in Eq. (3). Nevertheless, E_A and C_A reflect the physicochemical acceptor parameters of the probe (chelates 1 and 2). However, E_B and C_B refer to the physicochemical donor parameters of the bromide complex, so E_A and C_A solvent parameters were used as an alternative.

The frequencies of d–d absorption transition band (ν_{max}) of the current chelates in various solvents (Table 3) are fitted in Eqs. (1)–(3). The overall picture which emerges from the MLRA based on K-T solvent descriptors and Gutmann's donor–acceptor concept is then considered followed by the unified solvent model proposed by Drago. The regression coefficients and constant values are shown in Table 4.

The data in Table 4 shows positive signs of π^* and α coefficients for all investigated Me_4en-chelates, whereas it negative for β-coefficient in case of perchlorate and nitrato-chelates (**1** and **2**) and positive for bromo-chelate. This indicates bathochromic shift of d–d transition with the increasing of dipolarity-polarizability (π^*) and hydrogen bond donor (α) of solvent. On contrast increasing of hydrogen bond acceptor (β) leads to hypsochromic shift in case of chelates **1** and **2** and bathochromic for bromo-chelate. Moreover, the positive slope obtained for the linear relationship of the α coefficients *versus* anions donor number: $\alpha = 2.14 + 1.18\ DN_X$, $r = 0.97$.

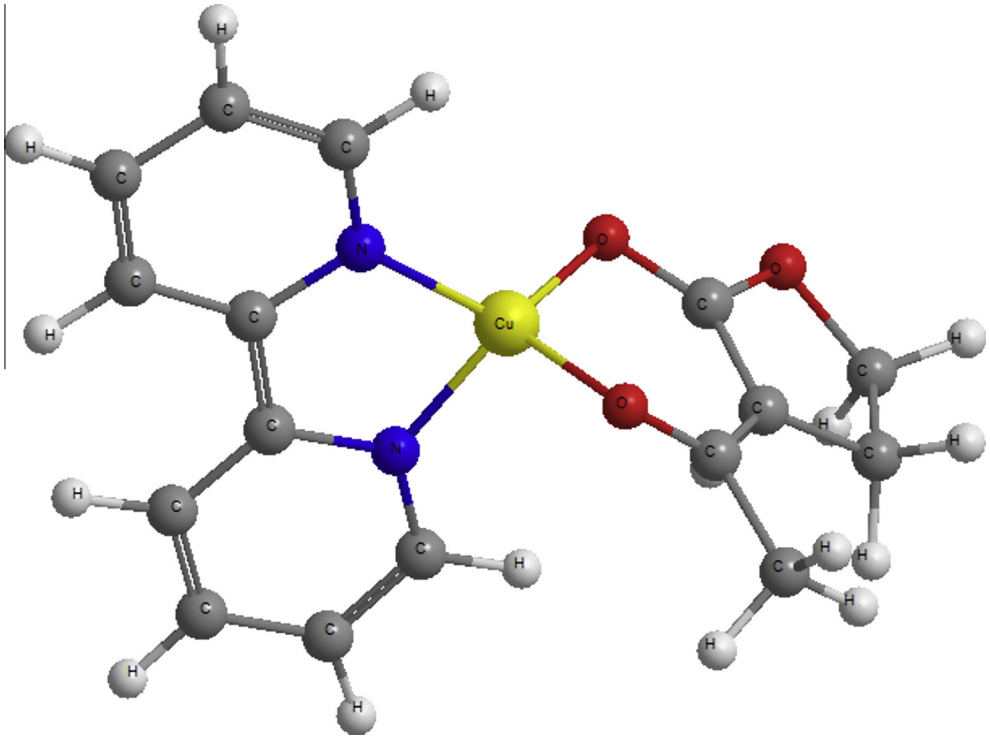

Fig. 5. Molecular modeling of $[Cu(AcBL)(Bipy)]^+$ (**3**).

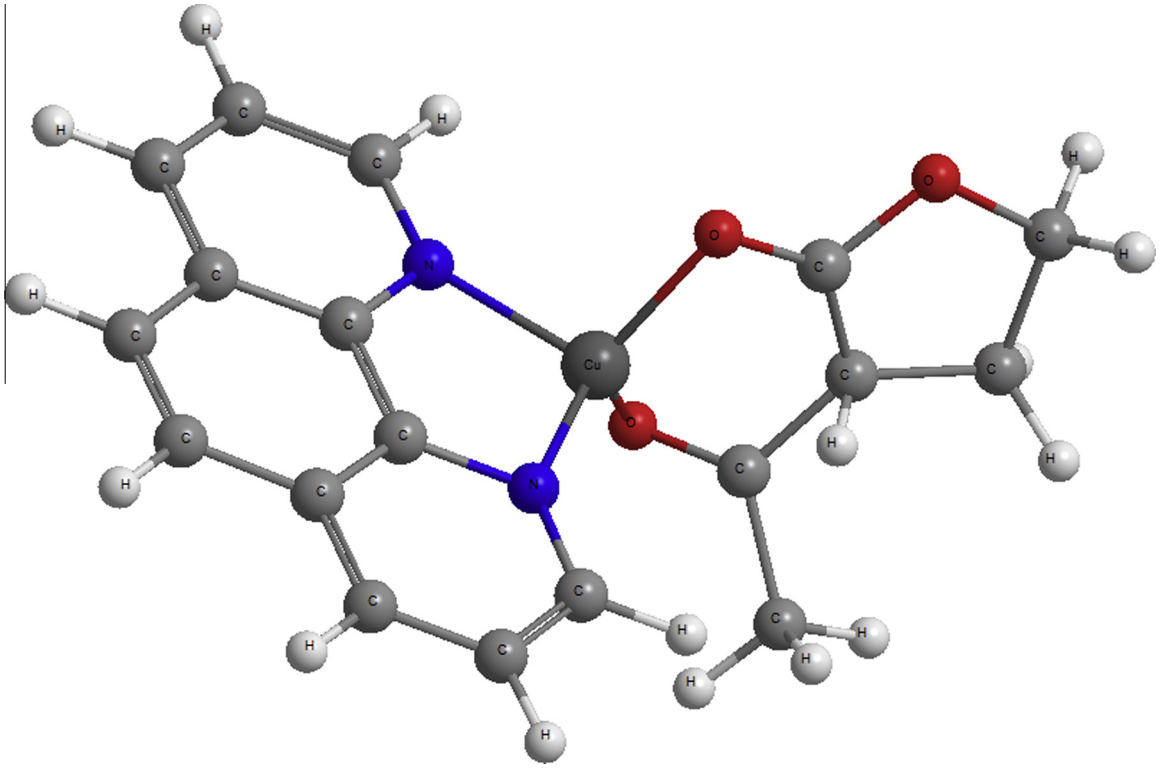

Fig. 6. Molecular modeling of $[Cu(AcBL)(Phen)]^+$ (**4**).

This in term indicates that the ground state (GS) of bromide complex is more polar than the excited state (ES), the observed solvatochromic shifts resulting from more polar solvents stabilizing the GS than the ES, leading to increase transition energy (blue shift).

Fitting of the spectral data in Table 3 in Eq. (2) indicates dependence of the d–d absorption transitions on the *DN* and *AN* parameters. The negative sign of the coefficient of the Lewis-basicity (a) reveals red shift, in contrast to the positive sign of the coefficient

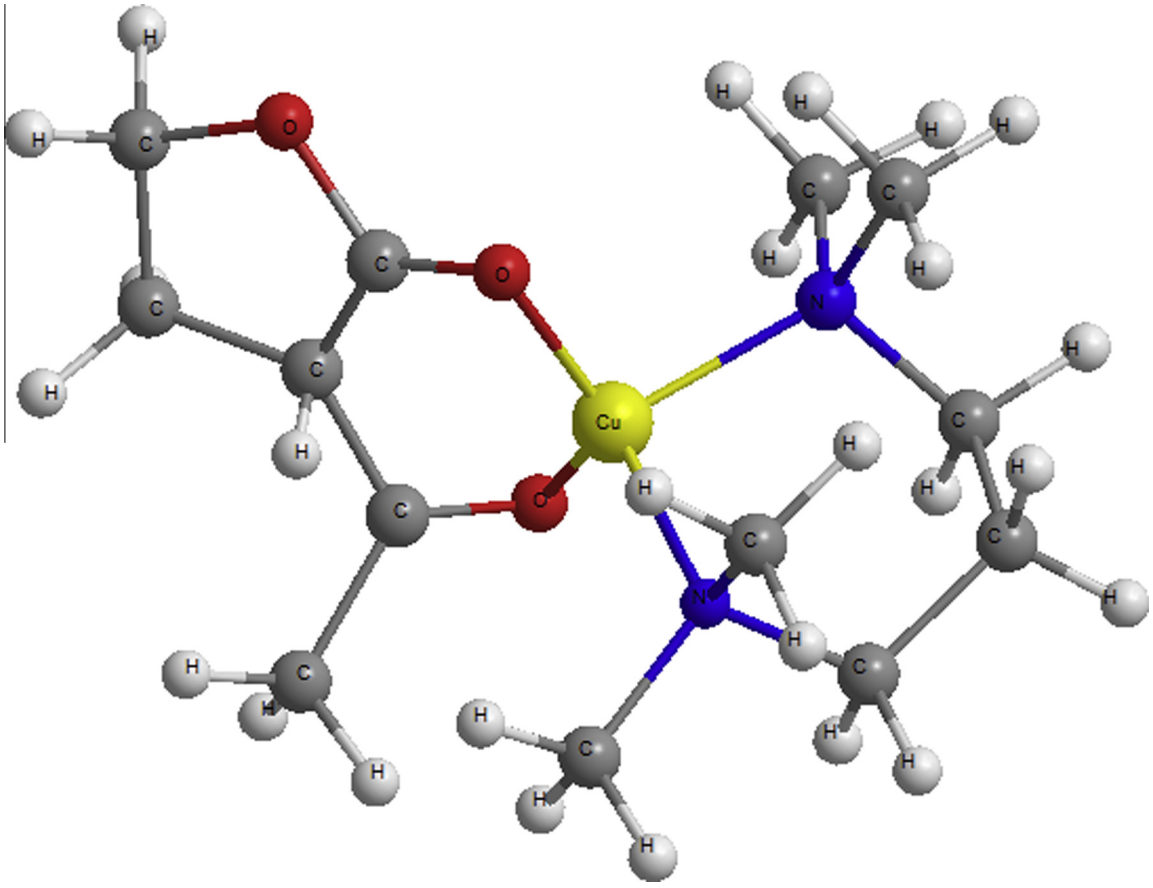

Fig. 7. Molecular modeling of $[Cu(AcBL)(Me_4Pn)]^+$ (**5**).

of Lewis-acidity (*b*) that indicates a blue shift. This reflects again the role of counter-anion on the type of solvatochromicity.

The relative percentage of the influences *DN* and *AN* parameters on the ν_{max} values were calculated from the coefficients of *a* and *b*, and found in the ranges 6.5–97.5% and 2.5–93.5.5%; for complexes **1** and **2**, respectively. The data in Table 4 suggests that the *DN* parameter of the solvent has the dominant contribution (89.4–97.5%) in the shift of d–d absorption band of the chelates **1** and **2**. However, in the case of bromide complex the contribution of *AN* parameter is more pronounced than the *DN* parameter (93.5% and 6.5%), respectively.

Finally, fitting the ν_{max} data in Table 3 in Eq. (3) indicates dependence of the observed spectral shifts on the dipolarity/polarizability parameter *S* and both components of the Lewis acid-base quantification, *E* and *C* parameters. The regression coefficients recognize that the specific solute–solvent interaction is more predominant in that influencing the shift of the d–d absorption transitions (contribution percentages, 70–77%). The two parts of the specific term, electrostatic (*E*) and covalent (*C*), are almost of similar importance for perchlorate and nitrate chelates. However, the contribution of *C* is more pronounced than *E* in case of bromide chelate.

The negative signs of *P*(*S*), *C* and *E* coefficients for chelates **1**–**2** refer to a positive solvatochromism (red shift). However, a negative solvatochromism (blue shift) is accomplished from the positive signs of *P*, *C* and *E* coefficients for the bromide chelate. This explanation is consistent with that obtained from treatment of the present data by K-T and Gutmann's models, Eqs. (1) and (2).

Therefore, relevant data were obtained by correlating the coefficients of *DN* and *AN* parameters, (*a*, *b*) terms, against either those of α, β and π^* or (*E* + *C*) coefficients (star on symbol was taken to refer its coefficient), from Table 4; $a = -0.06 + 0.24\ \beta$, $r = 0.99$; $b = -0.19 + 0.35\ \alpha$, $r = 1.0$; $b = -0.08 + 0.33\ C$, $r = 1.0$; and $\pi^* = 0.83 + 0.71\ (E + C + P)$, $r = 1.0$. These linearities further support stabilization of the ground state of the probe through donor–acceptor interactions with the solvent molecules [10].

The results discussed above clarify by considering specific interactions of the investigated chelate with the lone pair of the donor solvent. The competition between solvent and anion to coordinate with the central metal ion should be considered as illustrated below (route i). The solvated species then dissociates depending on the solvent polarity (non-specific), (route ii). This is indicated from the relative contribution percentage of specific (70–77%) and non-specific (23–30%) terms as shown in Table 4.

$$Cu(AcBL)(Me4en)X + n\ S \rightleftharpoons Cu(AcBL)(Me4en)(S)nX \quad \text{(i)}$$

$$Cu(AcBL)(Me4en)(S)nX \rightleftharpoons [Cu(AcBL)(Me4en)(S)n]^+ + X^- \quad \text{(ii)}$$

where, S refers to the solvent molecule.

The d–d band frequencies (ν_{max}) of the current chelates $[Cu(AcBL)(L)]ClO_4$ in Nujol mulls given in Table 1, reflect the effect of equatorial ligands on the position of d–d band, Me_4en > Bipy ≈ Phen > Me_4pn, 17,094, 16,103, 16,077 and 14,836 cm^{-1}. This is emphasized by the linear correlation of the UV/Vis spectral data of the complexes *versus* the structural parameters of the current compounds (*vide infra*).

4. Molecular orbital calculations

Quantum chemical calculations were conducted and also to provide molecular-level understanding of the observed experimental behavior. All quantum chemical properties were obtained after geometric optimization using semiempirical at *PM3* level implemented by the *hyperchem 7.52* program. Figs. 3–8 show fully

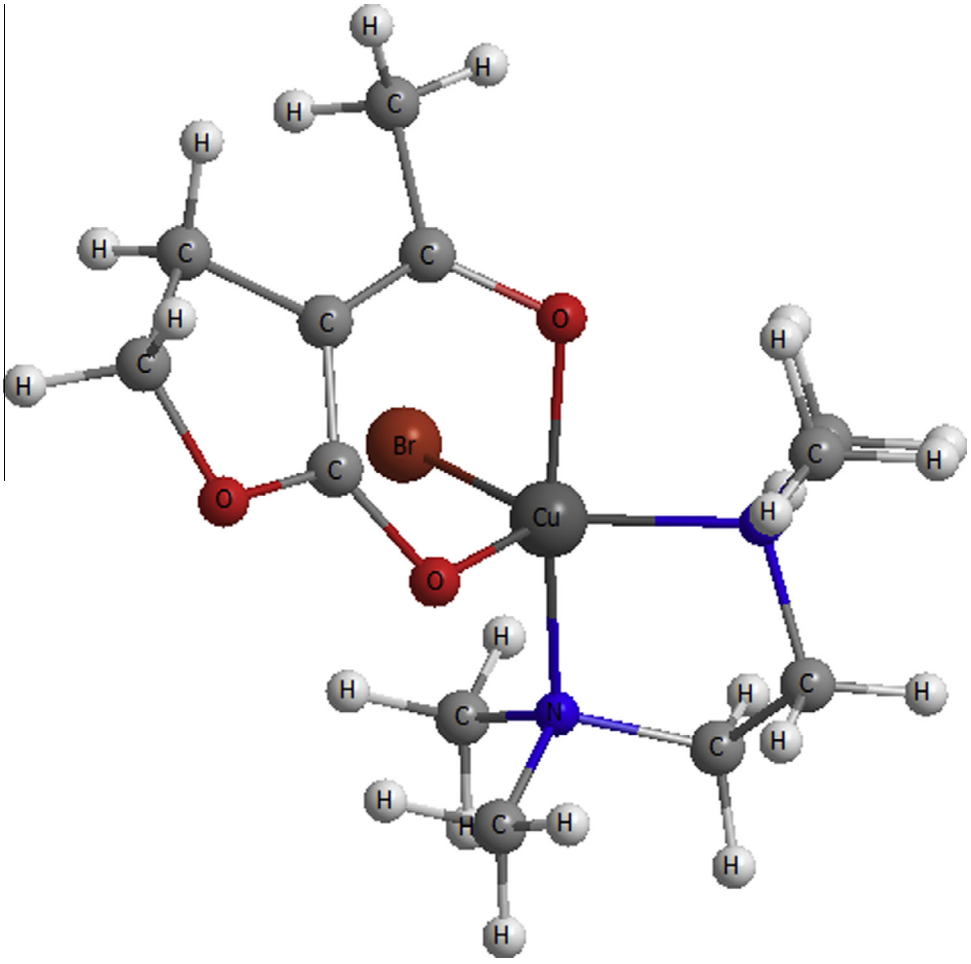

Fig. 8. Molecular modeling of [Cu(AcBL)(Me_4en)Br] (**6**).

Table 5
Structural parameters of the current free ligands.

Property	Heat of Formation, kcal/mol	Dipole moment	HOMO Energy, [EV]	LUMO Energy, [EV]	E_{gap}
Ligands					
HAcBL	−129.00	2.17	−11.19	−0.24	11.43
Me_4en	−13.91	1.57	−9.00	−2.39	11.39
Me_4pn	−19.24	2.18	−9.05	2.45	11.50
Bipy	62.39	0.003	−9.33	−0.71	8.62
Phen	71.30	3.00	−9.15	−0.84	8.31

optimized structures of the proposed structures those elucidated on the basis of analytical and spectral data of the current chelates. Various computed quantum chemical indices such as the energies of the lowest unoccupied (E_{LUMO}) and highest occupied molecular orbitals (E_{HOMO}) and E_{gap} ($E_{gap} = E_{Lumo} - E_{HOMO}$) and dipole moment ($\mu$) of the ligands and their complexes are listed in Table 6. Frontier orbital theory is useful in predicting the extent of interaction between ligands and metal ion. Terms involving the frontier molecular orbital could provide dominative contribution, because of the inverse dependence of stabilization energy on orbital energy difference [29]. Moreover, the gap between the HOMO and LUMO energy levels of the molecules was another important factor that should be considered.

Structural parameters of the free ligands and their complexes given in Tables 5–7, are correlated with the current experimental data. E_{LUMO} and E_{gap} of the free N–N ligands *versus* UV/Vis spectral data (ν_{max}) of the complexes in Nujol mulls yielding: E_{gap}/eV = −38.17 + 0.0032 ν_{max}, $r = 0.99$ (3 points except Me_4pn) and E_{LUMO}/eV = −51.52 + 0.0032ν_{max}, $r = 0.99$ (3 points except Me_4pn). The positive slopes reveal that the increase of either E_{gap} or E_{LUMO} of the free N–N ligand leads to increase the ligand field stabilization energy (*LFSE*) of the formed mixed chelate of Cu(II).

E_{HOMO} of copper(II)-chelates *versus* $\nu_{C=O}$; E_{HOMO} = −25.07 + 0.011 $\nu_{C=O}$, $r = 0.99$ ($n = 4$, except chelate **2**), shown in Fig. 9(A). The positive slope of this correlation refers to the increase of E_{HOMO} (less stable) with the increase of the bond strength of C=O, i.e., decrease the bond strength of ν(Cu–O). This explanation is emphasized by the negative slope of the linear correlation of E_{gap} *versus* $\nu_{C=O}$; E_{gap} = 30.46–0.015 $\nu_{C=O}$, $r = 0.95$, ($n = 4$ except chelate **2**). The linearity indicates increase of the bond strength of carbonyl

Table 6
Structural parameters data of free HAcBL ligand and its mixed ligand complexes, calculated on the basis of semi-emperical *PM3* level implemented on *Hyperchem 7.52* program.

Property/ Complex	1	2	3	4	5	6
Total energy (kcal/mol)	−96,140	−123,560	−104,210	−109,678	−99,584	−104,298
Binding energy (kcal/mol)	−3931	−4530	−4152	−4489	−4206	−3959
Electronic energy (kcal/mol)	−642,960	−943,555	−687,300	−763,800	−696,236	−702,032
Heat of formation (kcal/mol)	−196	−229	−151	−147	−196	−198
Dipole moment (D)	7.66	8.83	−5.62	8.06	6.81	5.71
HOMO (eV)	−7.01	−3.65	−7.54	−7.17	−7.22	−7.52
LUMO (eV)	−1.33	0.57	−1.21	−1.53	−1.48	−0.41
Polarizability	30.07	27.8	30.07	32.77	25.66	26.84
Hydration energy	−10.76	−7.67	−10.76	−10.35	−3.58	−2.49

Table 7
Calculated the bond lengths (A°) of the free HAcBL ligand and its complexes.

Compound	C=O	M–O_L	M–N	M–O=C	M–Br
HAcBL	1.21	–	–	–	–
1	1.23	1.95	1.95	1.91	–
2	1.27	1.95	1.97	1.91	–
3	1.27	1.89	1.90	1.93	–
4	1.34	1.84	1.92	2.05	–
5	1.33	1.96	2.00	2.30	–
6	1.49	1.90	1.93	1.89	2.3

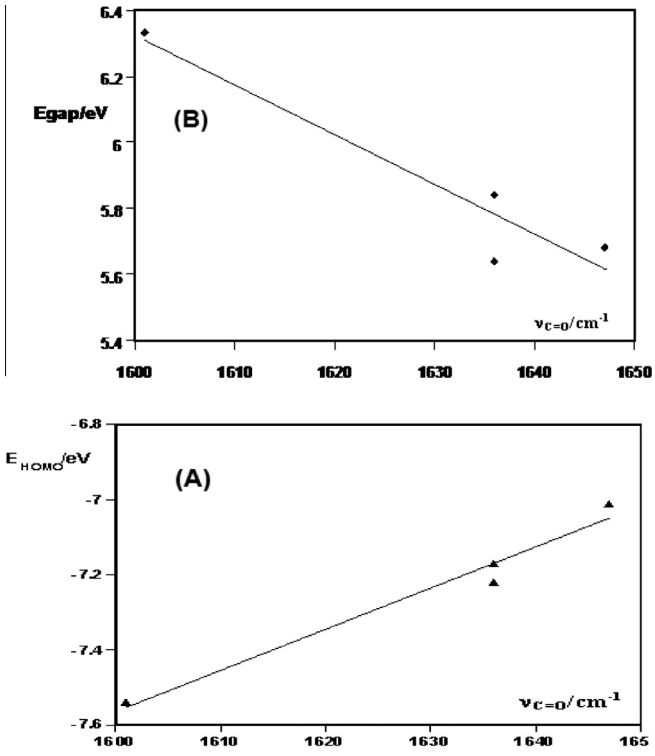

Fig. 9. The relationships of E_{HOMO} *versus* $\nu_{C=O}$ (A) and ΔE_{gap} *versus* $\nu_{C=O}$ (B).

group (νC=O) with the decrease of E_{gap} (see insert in Fig. 9(B)), i.e., as the strong interaction between the carbonyl of HAcBL free ligand and copper(II) increases, the bond strength of C–O will decreases (lowering the stretching frequencies of the free ligand); the stronger the M–O bond, the weaker the C–O bond, consequently E_{gap}, which corresponding to the *LFSE* of the chelate, increases.

This interpretation agrees well the first bond length Gutmann's variation rule [30] "expresses the inverse relationship between inter-molecular and intramolecular bond lengths adjacent to the sites of interaction". The Cu–O distances may be considered as intermolecular, by which the adjacent C–O bonds affected; the shorter the Cu–O bond (strong interaction), the longer the C–O bond (weaker) [22]. This conclusion is further confirmed by the negative slope (inverse relationship) of the linear correlation of the calculated bond lengths of carbonyl group and M–O with their IR frequencies of the current chelates, C–O (bond length) = 22.33–0.013 $\nu_{C=O}$, $r = 0.97$ ($n = 4$, except chelate **3**) and M–O bond length = 12.12–0.0227 ν_{M-O}, $r = 0.96$ ($n = 4$, except chelate **2**).

The linear correlation of the IR frequencies of Cu–O with the calculated dipole moment (μ/D) of the prepared chelates (Table 5), $\mu/D = 63.68–0.128\ \nu_{M-O}$, $r = 0.94$, $n = 4$, except chelate **4**. The negative slope recommends decreasing of the dipole moment with the increasing of M–O bond strength (higher frequencies). This finding concurs with the results obtained for related copper(II) and nickel(II) chelates [2,31,32].

4. Conclusion

A newly solvatochromic mononuclear mixed ligand Cu(II)-chelates have been synthesized and characterized on the basis of spectral, conductance and magnetic measurements. Studies on the complexes were carried out in solution proposing the plausible structure, Cu(AcBL)(L)X, based on the free solubility in most solvents. The UV–vis spectra on the solution of the copper(II)-complexes in various solvents found to be depend upon the type of solvent (solvatochromic, change of color from violet to green as the Lewis basicity of the donor solvent increases). The d–d absorption bands of Me_4en-chelates as Nujol mulls or in weak donor solvents revealed square-planar, and distorted trigonal bipyramid geometries for the perchlorate, and either for nitrate or bromide chelates, respectively. Specific and non-specific interactions of solvent molecules with the chelates were investigated using the unified solvation model. The plausible proposed structures of the chelates were optimized using hyperchem 7.5 program and the structural parameters were calculated and correlated with the experimental data.

References

[1] W. Linert, Y. Fukuda, A. Camard, Coord. Chem. Rev. 218 (2001) 113–152.
[2] A.A. Soliman, A. Taha, W. Linert, Spectrochim. Acta A 64 (2006) 1058–1064.
[3] I. Kuzniarska-Biernacka, A. Bartecki, K. Kurzak, Polyhedron 22 (2003) 997–1007.
[4] H. Golchoubian, G. Moayyedi, G. Bruno, H.A. Rudbari, Polyhedron 30 (2011) 1027–1034.
[5] H.P. Rang, M.M. Dale, J.M. Ritter, Pharmacology, third ed., Churchill Livingstone, 1995.
[6] E.A.M. Badawey, I.M. El-Ashmawey, Eur. J. Med. Chem. 33 (1998) 349–361.
[7] E.A.M. Badawey, T. Kappe, Eur. J. Med. Chem. 32 (1997) 815–822.
[8] Y. Fukuda, K. Sone, Inorganic Thermochromism Inorganic Chemistry Concept, Springer, Berlin, 1987. 10.
[9] A. Taha, Synth. React. Inorg. Metal Org. 31 (2001) 227–238.
[10] A. Taha, New J. Chem. 25 (2001) 853–858.
[11] A. Taha, Spectrochim. Acta A 59 (2003) 1373–1386.
[12] A. Taha, Spectrochim. Acta A 59 (2003) 1611–1620.

[13] W. Linert, A. Taha, J. Coord. Chem. 29 (1993) 265–276.
[14] F.E. Mabbs, D.I. Machin, Magnetism and Transition Metal Complexes, Chapman and Hall, London, 1973.
[15] HyperChem version 7.5 Hypercube Inc, (2003).
[16] K. Nakamoto, Infrared Spectra of Inorganic and Coordination Compounds, 5th edn., John Willey & Sons, New York, 1997.
[17] H. Golchoubia, E. Rezaee, J. Mol. Struct. 929 (2009) 154–158.
[18] O.M.I. Adly, Spectrochim. Acta A 95 (2012) 483–490.
[19] M. Shebl, J. Coord. Chem. 62 (2009) 3217–3231.
[20] W.J. Geary, Coord. Chem. Rev. 7 (1971) 81–122.
[21] W. Linert, R.F. Jameson, A. Taha, J. Chem. Soc. Dalton Trans. (1993) 3181–3186.
[22] Y. Marcus, Chem. Soc. Rev. (1993) 409–416.
[23] A. Taha, Monatsh. Chem. 125 (1994) 1189–1196.
[24] J.A. Kamlet, J.L.M. Abboud, M.H. Abraham, R.W. Taft, J. Org. Chem. 48 (1983) 2877–2887.
[25] C. O'Sullivan, G. Murphy, B. Murphy, B. Hathaway, J. Chem. Soc. Dalton Trans. 2 (1999) 1835–1839.
[26] R.S. Drago, Coord. Chem. Rev. 33 (1980) 251–277.
[27] R.S. Drago, D.C. Ferris, N. Wong, J. Am. Chem. Soc. 112 (1990) 8953–8961.
[28] R.S. Drago, J. Chem. Soc., Perkin Trans. 2 (1992) 1827–1838.
[29] O. Exner, Correlation Analysis of Chemical Data, Plenum Press/SNTL, New York/Prague, 1988.
[30] V. Gutmann, The Donor–Acceptor Approach Molecular Interactions, Plenum Press, New York, London, 1978.
[31] J. Fang, J. Li, J. Mol. Struct. THEOCHEM 593 (2002) 179–185.
[32] W. Linert, A. Taha, J. Chem. Soc. Dalton Trans. (1994) 1091–1095.